On *a posteriori* Error Estimation in Low-Frequency Computational Electromagnetics: Reflections on Historical Foundations, Current Realities, and Data-Driven Needs

***Abstract* — This article offers a reflection on *a posteriori* error estimation in low-frequency computational electromagnetics as an essential tool for solution credibility. While mesh-based error analysis for potential formulations matured decades ago, abundant computing power temporarily reduced interest in adaptive mesh refinement. Today, the rise of digital twins, surrogate modeling, and neural networks creates a strong demand for error estimation. Data-driven models increasingly benefit from clean and trustworthy training datasets, supported by quantitative measures of numerical error and uncertainty when demanded by the application. Classical error estimation principles are reviewed, with discussion of how tools once considered computationally burdensome are regaining relevance for automated data-quality certification, while practical perspectives are offered for future researchers navigating this domain.**

I. From classical FEM to error estimation

Numerical simulation based on the finite element method (FEM) is a standard and essential tool in low-frequency computational electromagnetics. The widespread adoption of FEM stems primarily from its flexibility in accommodating complex geometries and inhomogeneous material domains.

The theoretical foundations of low-frequency formulations were largely established during the peak period of potential formulation development in the 1980s and 1990s. During those decades, the rigorous derivation of dual potential formulations, the introduction of Whitney and Nédélec vector edge elements conforming to $H(\mathbf{curl})$, and appropriate topological gauging techniques provided the core mathematical framework for discrete electromagnetic field computations.

Over the subsequent decades, the focus within the computational electromagnetics community has naturally evolved toward practical extensions, engineering adaptations, and algorithmic refinements. These include nonlinear solver stabilization, specialized iterative linear solvers, numerical homogenization techniques for multiscale structures, as well as the formulation of multiphysics couplings, such as magneto-thermal or magneto-mechanical interactions. Furthermore, considerable attention has been directed toward downstream computational workflows, leveraging full-order finite element solutions to construct reduced-order models and surrogate models for efficient optimization, real-time control, and uncertainty quantification.

This methodological progress has been translated into practice through a diverse software ecosystem, ranging from commercial CAE packages to dedicated research platforms and open-source scientific software. In recent years, evolving geopolitical conditions and heightened corporate data security concerns have further intensified the focus on software sovereignty and IP protection. As a result, both industrial enterprises and research institutions are increasingly compelled to re-implement and maintain independent finite element solvers.

Yet, this widespread re-implementation of solver engines primarily aims at reproducing established numerical capabilities rather than fundamentally changing the underlying numerical theory. While software architectures, user interfaces, and execution platforms continue to modernize, the underlying mathematical foundations remain firmly anchored in the core formulations established decades ago.

When using numerical simulations for critical engineering decisions, a fundamental question arises: *how accurate is the computed field, and to what extent can the results be trusted?* Answering this requires recognizing that numerical modeling is inherently a trade-off between finite computational resources and the physical accuracy required for design. Because fully resolved modeling is generally computationally prohibitive, approximations are unavoidable at every stage of the numerical pipeline.

At the highest level, an engineer introduces physical and geometric idealizations. These choices include whether to account for multiphysics couplings (e.g., magneto-thermal interactions), whether to reduce a 3D geometry to 2D, whether to omit small structural features like fillets, and how to model complex regions such as laminated iron cores or stranded windings via continuum homogenization. Material models also add discrepancies through measured $\mathbf{B} - \mathbf{H}$ curves, anisotropy, and hysteresis losses. These choices depend entirely on engineering judgment and physical insight; numerical algorithms cannot, by themselves, detect or correct flawed modeling assumptions.

Once the underlying physics is translated into a governing mathematical formulation (e.g., partial differential equations in space and time), different sources of uncertainty and numerical error enter the solution process. These discrepancies arise from distinct sources:

1. *Parameter Uncertainties:* Material or geometric variabilities are addressed using uncertainty quantification (UQ) or stochastic methods, which reformulate the nondeterministic system into a sequence of deterministic computations.
2. *Algebraic Solver Residuals:* Discrepancies arising from nonlinear iterations (e.g., Newton–Raphson) and linear solver tolerances can generally be reduced substantially by imposing tighter convergence criteria, subject to conditioning and finite-precision limitations.
3. *Discretization Errors:* Arising from both spatial meshing and time-stepping schemes, discretization errors are different from solver residuals. Once the spatial mesh and temporal mesh are generated, the discretization error becomes inherently embedded in the discrete solution and cannot be reduced by further algebraic iterations.

Comparing these mechanisms reveals a clear mathematical hierarchy. Once the spatial (and, where applicable, temporal) discretization is established, the discrete approximation space V_h is fixed. For a given continuous problem, the accuracy that can be achieved within this space is therefore limited by its approximation capacity; tighter solver tolerances cannot overcome this discretization limit. Similarly, while increasing the number of parameter samples reduces statistical sampling errors, it does

not alter the underlying spatial approximation space of each deterministic sample. Therefore, controlling discretization error provides an important component of numerical verification.

While classical *a priori* error estimates confirm asymptotic convergence as the global mesh size $h \to 0$, uniform refinement in 3D problems causes the degrees of freedom to scale as $O(h^{-3})$, quickly overwhelming computational memory and compute time. Historically, engineers attempted to bypass this by manually refining elements near obvious features like air gaps or skin depth layers based on intuition. While practical for simple 2D cases, this manual approach is inherently flawed in complex 3D systems: field gradients and flux paths cannot be reliably predicted prior to solving. As a result, heuristic meshing routinely over-refines uncritical regions while under-refining true error-concentrated areas, offering no mechanism to measure or guarantee solution accuracy. To overcome the inherent unpredictability of engineering heuristics, a fundamentally different paradigm is required: one that replaces intuitive guesswork with a mathematically rigorous framework capable of quantifying and localizing discretization errors.

To establish a rigorous mathematical foundation for quantifying discretization errors, we consider the abstract variational formulation of the governing boundary value problem. Let V be a Hilbert space over a domain D (defined over $\mathbb{R}$, or $\mathbb{C}$ for time-harmonic formulations), equipped with a norm $\|\cdot\|_V$ tailored to the specific problem. The continuous problem seeks $u \in V$ such that:

$$a(u, v) = L(v) \quad \forall v \in V, \tag{1}$$

where $a(\cdot,\cdot) : V \times V \to \mathbb{R}$ (or $\mathbb{C}$) is a continuous and coercive bilinear (or sesquilinear) form, and $L(\cdot) \in V'$ is a bounded linear (or antilinear) functional representing source terms and boundary conditions.

Upon establishing a conforming finite-dimensional subspace $V_h \subset V$ associated with a mesh $\mathcal{T}_h$, the Galerkin discrete approximation seeks $u_h \in V_h$ satisfying:

$$a(u_h, v_h) = L(v_h) \quad \forall v_h \in V_h. \tag{2}$$

The discretization error is defined as $e = u - u_h \in V$.

The distinction between *a priori* and *a posteriori* error estimates lies primarily in the information on which the estimates depend. Classical *a priori* analysis yields estimates of the form:

$$\|u - u_h\|_V \leq C\, h^p\, \eta(u). \tag{3}$$

Equation (3) provides the mathematical justification for traditional uniform mesh refinement: for sufficiently smooth solutions, global refinement (the mesh size $h \to 0$) guarantees error reduction. However, the bound requires the unknown exact solution u to construct the quantity $\eta(u)$ and also involves the unknown constant C. Therefore, *a priori* bounds generally cannot be directly evaluated for a particular discrete solution and do not provide a fully computable error bound.

Babuška and Rheinboldt pioneered the theoretical foundations of finite element error estimation, establishing that meaningful quantitative error control must rely on computable bounds derived directly from the numerical solution itself [1]. In an ideal mathematical setting, one would seek an estimator $\eta(u_h)$ equal to the exact discretization error, i.e., $\eta(u_h) = \|u - u_h\|_V$. However, computing the exact error norm is practically infeasible, as it inherently requires knowledge of the unknown solution u. As a necessary compromise, *a posteriori* error analysis constructs a fully computable estimator $\eta(u_h)$, derived solely from u_h and problem data (a, L), that is norm-equivalent to the exact error up to two positive constants C_1 and C_2:

$$C_2\, \eta(u_h) \leq \|u - u_h\|_V \leq C_1\, \eta(u_h), \tag{4}$$

where C_1 and C_2 are positive constants independent of the mesh size h.

The dual requirements of reliability and efficiency determine the practical utility of the estimator:

1. *Reliability (Upper Bound):* Controlled by the constant C_1, the upper bound

$$\|u - u_h\|_V \leq C_1\, \eta(u_h), \tag{5}$$

guarantees that the estimated error securely bounds the true discretization error from above. This prevents underestimating numerical errors, providing the mathematical certificate required for engineering verification.

2. *Efficiency (Lower Bound):* Controlled by the constant C_2, the lower bound $C_2\, \eta(u_h) \leq \|u - u_h\|_V$, or equivalently,

$$\eta(u_h) \leq C_2^{-1} \|u - u_h\|_V, \tag{6}$$

prevents the estimator from overestimating the exact error. When localized to individual elements $T \in \mathcal{T}_h$, efficiency ensures that $\eta_T(u_h)$ faithfully tracks the spatial error distribution, serving as a reliable indicator to drive adaptive mesh refinement.

When an estimation technique achieves $C_1 = 1$ without uncomputable asymptotic constants or saturation assumptions, it delivers a guaranteed upper bound, providing inherent mathematical certainty for solution verification.

II. Methodological reflections on error estimation in low-frequency computational electromagnetics

A. Early attempts with heuristic error indicators

Apart from mathematical developments within the formal error estimation framework, early low-frequency computational electromagnetics saw numerous practical explorations long before these rigorous concepts were widely applied. Driven by engineers and applied physicists, these early efforts were guided by physical intuition regarding real-world device behavior, such as magnetic saturation, steep air-gap gradients, interface boundary conditions, and skin depth effects. It should be explicitly noted that the historical examples mentioned here are not intended to serve as an exhaustive survey of the state of the art; omitting specific early contributions in no way diminishes their historical value. Instead, this selection illustrates how early adaptive mesh refinement naturally originated from physically observable quantities, such as stored magnetic energy, co-energy, and local field continuity across material boundaries.

Early self-adaptive meshing strategies arose directly from simple, intuitive field observations. Penman and Grieve [2] were among the first to use local magnetic energy density variations and potential gradients as direct proxies for discretization errors. Focusing on physical boundary behavior, Hahn et al. [3] and Raizer et al. [4] recognized that finite element discretization artificially breaks field continuity, using the nonzero jumps in normal flux density $\mathbf{B}_n$ and tangential field intensity $\mathbf{H}_t$ across element interfaces to drive mesh adaptation.

In parallel, researchers explored various local procedures to assess solution quality. Fernandes et al. [5] evaluated local error

strategies for static and quasi-static formulations, expanding on local potential formulations [6] that were later adopted by Drago et al. [7] for local potential solves and refinement. Extending these ideas to 3D magnetostatics, Nehl and Field [8] combined field gradient metrics with local Delaunay subdivisions for first-order tetrahedral meshes. As these practical criteria multiplied, comparative studies emerged to evaluate their real-world performance. For instance, Labridis [9] systematically benchmarked various adaptive mesh refinement criteria for multi-conductor eddy-current problems, showing how heavily engineering practice relied on metrics like skin depth and power loss gradients.

In low-frequency applications, engineers kept using physical metrics instead of abstract mathematical norms for a long time. Even as late as the 2000s, Ladas et al. [10] derived adaptive meshing criteria directly from thermodynamic principles and energy or co-energy variations, reiterating that stored electromagnetic energy remains the most natural quality metric for electrical engineers. Strictly speaking, because these early formulations lack formal proofs for reliability, efficiency (see (5) and (6)), or guaranteed upper bounds, they fall under the mathematical taxonomy of error *indicators* rather than error *estimators*. Nevertheless, they provided practical guidance for mesh adaptation. In fact, many of these physical quantities, including interface jump conditions and local energy variations, reappear naturally within the mathematical terms of modern, rigorously proven error estimators.

B. Equilibrated error estimators based on non-verification of constitutive relations

Transitioning from heuristic error indicators to rigorous mathematical frameworks for error estimation, equilibrated error estimators stem from the Prager–Synge Hypercircle theorem [11], serving as a classical and rigorous foundation for error estimation. This methodology was pioneered by Ladevèze [12], who introduced the constitutive relation error (CRE) concept, formulating a general framework for verification by directly measuring the non-verification of material constitutive laws.

To illustrate this framework, consider for simplicity a magnetostatic problem posed over a bounded domain $D \subset \mathbb{R}^3$. Given a divergence-free source current density $\mathbf{J}_\mathrm{s}$, the governing field equations read:

$$\mathbf{curl}\ \mathbf{H} = \mathbf{J}_\mathrm{s}, \tag{7a}$$

$$\operatorname{div} \mathbf{B} = 0, \tag{7b}$$

$$\mathbf{B} = \mu \mathbf{H}, \tag{7c}$$

where $\mathbf{H}$ is the magnetic field intensity, $\mathbf{B}$ is the magnetic flux density, and μ is the magnetic permeability tensor. Equations (7a) and (7b) express Ampère's law and Gauss's law for magnetism, while (7c) is the constitutive relation.

To evaluate numerical accuracy, the CRE framework relies on constructing an admissible field pair $(\mathbf{H}^*, \mathbf{B}^*)$, wherein each component strictly satisfies its corresponding field topology:

$$\mathbf{curl}\ \mathbf{H}^* = \mathbf{J}_\mathrm{s} \quad \text{and} \quad \operatorname{div} \mathbf{B}^* = 0 \quad \text{in } D. \tag{8}$$

The core strength of the Hypercircle theorem lies in the exact orthogonality between solenoidal and irrotational error fields. For any admissible pair $(\mathbf{H}^*, \mathbf{B}^*)$, the exact solutions $(\mathbf{H}, \mathbf{B})$ obey the strict energy identity:

$$\|\nu^{1/2}(\mathbf{B}-\mathbf{B}^*)\|_D^2 + \|\mu^{1/2}(\mathbf{H}-\mathbf{H}^*)\|_D^2 = \|\nu^{1/2}(\mathbf{B}^*-\mu\mathbf{H}^*)\|_D^2, \tag{9}$$

where $\nu = \mu^{-1}$ is the magnetic reluctivity. Since all terms on the left-hand side are non-negative, (9) directly yields two fully computable, guaranteed upper bounds on the individual field errors without any uncomputable constants:

$$\|\mu^{1/2}(\mathbf{H}-\mathbf{H}^*)\|_D \le \|\nu^{1/2}(\mathbf{B}^*-\mu\mathbf{H}^*)\|_D, \tag{10a}$$

$$\|\nu^{1/2}(\mathbf{B}-\mathbf{B}^*)\|_D \le \|\nu^{1/2}(\mathbf{B}^*-\mu\mathbf{H}^*)\|_D. \tag{10b}$$

The adaptation of these fundamental principles within computational electromagnetics has progressed through systematic methodological extensions. Early investigations primarily focused on 2D heuristic adaptive mesh refinement and foundational self-adaptive mesh generation strategies for magnetic fields [13, 2]. As computational demands extended toward three-dimensional domains, these mesh adaptation techniques were successfully generalized to 3D finite element calculations alongside the development of local element-by-element error estimation methods [14, 15].

Concurrently, researchers began exploring complementary formulations and dual-field descriptions to better handle complex electromagnetic phenomena, particularly in nonlinear magnetostatic boundary value problems [16, 17, 18]. A decisive methodological bridge was subsequently forged by integrating constitutive relation error principles and projection-reconstruction techniques into magnetic field error estimation [19, 20].

Building upon these conceptual frameworks, the foundational and systematic development of dual systems and energy-based error bounds largely matured by around 2010. Energy approaches were established to systematically derive various dual formulations in magnetostatics [21], paving the way for reliable error estimators tailored for 3D linear magnetostatic problems [22], with further insights into dual-mesh complementarity established during that era [23]. Following this mature foundation, subsequent efforts have naturally branched into more specialized, incremental refinements—such as unstructured mesh scalar potential formulations via discrete geometric methods [24], algebraic topological frameworks like lean and one-stroke complementarity [25, 26], computational efficiency enhancements through shared finite element matrices motivated by the resurgence of direct solvers [27, 28], and extensions to multiscale finite element modeling across 2D and coupled 2D/1D contexts [29, 30, 31].

To better understand the implementation and performance of equilibrated error estimators, it is instructive to take standard potential formulations as a representative example. In the community of low-frequency computational electromagnetics, direct field formulations are rarely employed nowadays; potential formulations are far more widely adopted due to their flexibility in accommodating excitation sources, as well as handling coupling interfaces between conducting and non-conducting domains in eddy-current settings.

The classical potential formulation solves for the magnetic vector potential $\mathbf{A}$ via:

$$\mathbf{curl}\,(\nu\ \mathbf{curl}\ \mathbf{A}) = \mathbf{J}_\mathrm{s} \quad \text{in } D, \tag{11}$$

from which the discrete magnetic flux density is evaluated as:

$$\mathbf{B}_h = \mathbf{curl}\ \mathbf{A}_h. \tag{12}$$

By construction, the discrete magnetic flux density $\mathbf{B}_h$ automatically verifies Gauss's law $\operatorname{div} \mathbf{B}_h = 0$. Complementarily, the dual formulation solves for the magnetic scalar potential Ω via:

$$\operatorname{div}(\mu\, \nabla\Omega) = \operatorname{div}(\mu \mathbf{H}_\mathrm{s}) \quad \text{in } D, \tag{13}$$

where $\mathbf{H}_\mathrm{s}$ denotes a prescribed source field satisfying $\mathbf{curl}\ \mathbf{H}_\mathrm{s} = \mathbf{J}_\mathrm{s}$. The discrete magnetic field intensity:

$$\mathbf{H}_h = \mathbf{H}_\mathrm{s} - \nabla\Omega_h, \tag{14}$$

then automatically satisfies Ampère's law $\mathbf{curl}\,\mathbf{H}_h = \mathbf{J}_s$.

Because $\mathbf{B}_h$ and $\mathbf{H}_h$ independently satisfy Gauss's law and Ampère's law, respectively, the pair $(\mathbf{H}_h, \mathbf{B}_h)$ directly constitutes a globally admissible pair $(\mathbf{H}^*, \mathbf{B}^*)$ without requiring post-processing or local field reconstruction. Substituting these discrete fields into (9) yields:

$$\|\nu^{1/2}(\mathbf{B}-\mathbf{B}_h)\|_D^2+\|\mu^{1/2}(\mathbf{H}-\mathbf{H}_h)\|_D^2 = \|\nu^{1/2}(\mathbf{B}_h-\mu\mathbf{H}_h)\|_D^2. \tag{15}$$

Equation (15) provides a fully computable, guaranteed upper bound on the total numerical error without requiring any uncomputable constants. However, two primary practical limitations arise when applying this global dual-solving strategy purely for field error estimation. On the one hand, the right-hand side of (15) measures the combined energy errors of both the primal and dual solutions simultaneously. When evaluating the accuracy of a single formulation, this cumulative quantity inherently overestimates the actual error of the individual solution. On the other hand, constructing this admissible pair requires two independent, global finite element solves ($\mathbf{A}$ and Ω formulations) over the domain D, incurring a substantial computational cost that becomes impractical for large 3D configurations.

Despite these practical shortcomings in direct field-error evaluation, dual formulation strategies have continued to attract strong interest in practical engineering applications. Taking the primal $\mathbf{A}$ formulation as an example, the guaranteed bound $\eta = \|\nu^{1/2}(\mathbf{B}_h - \mu\mathbf{H}_h)\|_D$ satisfies

$$\|\nu^{1/2}(\mathbf{B} - \mathbf{B}_h)\|_D \leq \eta. \tag{16}$$

While the triangle inequality yields

$$\|\nu^{1/2}\mathbf{B}\|_D \leq \|\nu^{1/2}\mathbf{B}_h\|_D + \eta, \tag{17}$$

this estimate is inherently conservative and far less sharp. Instead, the primary appeal of dual formulations lies in their ability to compute sharp, complementary bounds directly on global lumped RLC parameters. As emphasized by Bossavit [32], this framework provides strict bilateral estimates for global quantities like energy, inductance, and capacitance in static situations, even though such guaranteed two-sided enclosures seem not to be supported by theory for eddy current cases.

However, this feature offers little help when it comes to adaptive mesh refinement. Practical adaptive mesh refinement relies on element-wise error indicators to guide local mesh refinement for a chosen primary solver. Because η reflects the combined discrepancy between the discrete spaces of $\mathbf{B}_h$ and $\mathbf{H}_h$, it fails to identify the localized error of either formulation individually. This lack of decoupling makes it an impractical local refinement metric for single-mesh adaptation.

C. Residual error estimators

To address the need for effective local indicators in adaptive mesh refinement, where element-wise information is required to guide mesh adaptation for a single solver, residual-based error estimators regained substantial attention during roughly the same period. Since solving two full numerical systems for dual formulations was computationally too expensive at that time, residual-based methods provided a practical alternative. Operating under a strict single-solve paradigm, their primary goal is to extract local discretization error information exclusively from the discrete solution of a single formulation, making them inherently suited for single-mesh adaptive refinement.

The mathematical foundations of residual-based error analysis were established by Babuška and Rheinboldt [1] in the context of structural mechanics. When translated to computational electromagnetics, early theoretical work naturally focused on field formulations solving directly for the electric field $\mathbf{E}$ or magnetic field $\mathbf{H}$, especially using edge elements. During the 2000–2010 period, notable contributions in this direction include, among others, [33, 34, 35, 36, 37].

In low-frequency computational electromagnetics, after years of extensive discussion and comparison among various field representations, potential formulations eventually emerged as the predominant choice. Formulations such as $\mathbf{A}$–φ and $\mathbf{T}$–Ω, along with their various variants, gained widespread adoption due to two major advantages over direct field $\mathbf{E}$ (or $\mathbf{H}$) formulations. On the one hand, while direct $\mathbf{E}$ (or $\mathbf{H}$) formulations are primarily tailored for conducting eddy current domains and encounter intrinsic difficulties when extended to non-conducting or pure magnetostatic regions, potential formulations naturally couple conducting and non-conducting domains across complex topological configurations. On the other hand, potential formulations accommodate diverse current source excitations, such as stranded coils, voltage-driven conductors, and total current constraints, with significantly higher flexibility and algorithmic robustness.

Despite these practical benefits, transitioning error analysis from field formulations to potential formulations is by no means trivial. Starting around 2010, a series of mathematical works emerged to establish rigorous error analysis specifically for potential formulations across magnetostatic and eddy current problems.

The primary mathematical hurdle lies in enforcing the gauge condition, which causes the discrete finite element space to become nonconforming ($V_h \not\subset V$), thereby rendering classical error analysis tools inapplicable. Intriguingly, however, key physical constraints inherent to electromagnetics, such as the divergence-free nature of the source current ($\nabla \cdot \mathbf{J}_s = 0$), can mathematically restore conformity by embedding the discrete problem into a suitably enriched space [38]. Furthermore, addressing the error spaces associated with different potential formulations necessitates tailoring specialized Helmholtz decompositions. These decompositions leverage fundamental projection properties to achieve sharp upper error bounds needed in the estimate.

Specifically, in the magnetostatic regime, the Ω formulation can be viewed as a direct extension of structural mechanics frameworks, as it reduces fundamentally to a Laplace-type scalar problem. In contrast, for the $\mathbf{A}$ formulation, dedicated residual error estimators were developed and rigorously compared against equilibrated error estimators [39].

For eddy current problems, mathematically rigorous residual error estimates for potential formulations were pioneered for the $\mathbf{A}$–φ formulation [38] and the $\mathbf{T}$–Ω formulation [40]. Concurrently, alternative potential representations, such as the $\mathbf{A}^*$ formulation, were also analyzed [41]. Subsequent theoretical advancements systematically resolved the challenges of handling mixed boundary conditions via adapted Helmholtz decompositions [42], incorporated diverse source excitation conditions [43], and extended the analysis to the time domain for eddy current problems [44], including joint space-time discretization error control [45].

These mathematical breakthroughs quickly drew significant interest from the computational electromagnetics community, initiating extensive engineering investigations and discussions grounded in physical intuition. Numerical studies reported comprehensive comparisons between residual and alternative estima-

tion techniques. For instance, residual estimators were evaluated side-by-side across both $\mathbf{A}$–φ and $\mathbf{T}$–Ω formulations [46], and compared with hierarchical error indicators in 2D eddy current problems [47]. The performance of these indicators within adaptive mesh refinement loops was further investigated [48]. Full physical configurations featuring distinct source excitation modes were systematically established [49], and residual estimators were later extended from low-frequency to intermediate-frequency regimes, such as the Darwin model [50]. Moreover, nonconforming finite element implementations were explored using residual-type estimators [51], alongside studies demonstrating the limitations of the traditional Zienkiewicz–Zhu (ZZ) patch recovery and advocating energy-based metrics for improved accuracy [52]. Finally, detailed comparative studies benchmarked residual estimators directly against equilibrated estimators for eddy current problems [53, 54].

To illustrate the performance of the residual-based error estimator in a manner parallel to the equilibrated estimator, we reconsider the magnetostatic problem using the $\mathbf{A}$ formulation defined in (12). With the numerical error in the energy norm $\|\nu^{1/2}(\mathbf{B}-\mathbf{B}_h)\|_D$, as in (16), denoted by $\varepsilon_{\mathbf{A},D}$, the local residual error estimator for an element T is defined as

$$\eta^2_{\mathbf{A},T} = \eta^2_{\mathbf{A};1} + \sum_{F\subset\partial T} \eta^2_{\mathbf{A};2}, \tag{18}$$

with

$$\eta^2_{\mathbf{A};1} = h_T^2 \left\|\mathbf{J}_\mathrm{s} - \mathbf{curl}\,(\nu\mathbf{B}_h)\right\|^2_T, \tag{19}$$

$$\eta^2_{\mathbf{A};2} = h_F \left\|[\nu\mathbf{B}_h\times\mathbf{n}]_F\right\|^2_F, \tag{20}$$

where $[\cdot]_F$ denotes the jump of a field quantity across the face F, $\mathbf{n}$ is the unit outward normal vector, and h_T and h_F represent the sizes of element T and face F, respectively.

Note that certain residual formulations in the literature explicitly include a data oscillation term for the source current density (e.g., $h_T\|\mathbf{J}_\mathrm{s}-\pi_h\mathbf{J}_\mathrm{s}\|_T$), where $\pi_h\mathbf{J}_\mathrm{s}$ denotes the discretization of $\mathbf{J}_\mathrm{s}$ in the Raviart–Thomas space. In potential-based formulations, ensuring $\mathrm{div}\,(\pi_h\mathbf{J}_\mathrm{s}) = 0$ is a strict prerequisite for the mathematical solvability and compatibility of the discrete system. Because this discrete representation of the source is rigorously constrained and resolved prior to the finite element solve, this higher-order oscillation term is neglected, and $\mathbf{J}_\mathrm{s}$ is directly used in the residual definitions.

Under this definition, the global reliability and local efficiency bounds are expressed as

$$\varepsilon_{\mathbf{A},D} \le C_1\,\eta_{\mathbf{A},D} \text{ with } \eta^2_{\mathbf{A},D} = \sum_{T\in\mathcal{T}_h}\eta^2_{\mathbf{A},T}, \tag{21}$$

and

$$\eta_{\mathbf{A},T} \le C_2^{-1}\,\varepsilon_{\mathbf{A},\omega_T}, \tag{22}$$

where the subscript ω_T denotes the patch of the element T, a subregion comprising element T and all its neighboring elements.

Unlike the equilibrated estimator, the reliability constant C_1 here remains unknown. Although C_1 is independent of both the mesh size h and the discrete solution, its indeterminacy prevents the residual estimator from providing a guaranteed upper bound for exact error control.

For local efficiency, however, the unknown constant C_2 poses no operational drawback in practice.

Because the efficiency constant is independent of the mesh size, the local indicator $\eta_{\mathbf{A},T}$ provides a mesh-independent relative measure of error concentration and can therefore be used to guide adaptive refinement. Furthermore, evaluating the interior and face residuals in (19)–(20) is computationally lightweight during post-processing; it can be readily accelerated via preassembled local matrices or parallelized across elements, avoiding the auxiliary global solver required by equilibrated estimators.

Examining the mathematical terms in (19)–(20) reveals a striking physical clarity that directly reflects the nature of weak formulation approximations by the FEM. The interior residual $\eta_{\mathbf{A};1}$ explicitly measures the violation of the strong-form governing equation inside each element T, which naturally arises because the FEM only satisfies the governing equation in a weak sense. Meanwhile, the interface jump term $\eta_{\mathbf{A};2}$ checks the discontinuity of the tangential magnetic field intensity $[\nu\mathbf{B}_h\times\mathbf{n}]_F$ across element faces.

Since standard conforming spaces cannot enforce strong tangential continuity for $\nu\mathbf{B}_h$ obtained by the $\mathbf{A}$ formulation, this term quantifies how well the discrete solution meets interface continuity, while on external domain boundaries, it verifies the weak enforcement of Neumann boundary conditions.

Mathematically, both the interior residual $\eta_{\mathbf{A};1}$ and the face jump term $\eta_{\mathbf{A};2}$ are indispensable for rigorously proving the reliability and efficiency bounds. In practice, however, when low-order edge elements are used, $\mathbf{B}_h = \mathbf{curl}\,\mathbf{A}_h$ is element-wise constant, leading to $\mathbf{curl}\,(\nu\mathbf{B}_h) = \mathbf{0}$ throughout the domain. Consequently, the interior residual simplifies to $h_T^2\|\mathbf{J}_\mathrm{s}\|^2_T$, indicating that the strong governing equation is never satisfied pointwise in source excitation regions, whereas it is trivially satisfied in source-free air regions regardless of the actual quality of the discrete solution. This structural degeneration from an error estimation perspective underscores a fundamental approximation bottleneck of low-order discretization: low-order elements provide less informative element-interior residuals, forcing refinement decisions to rely predominantly on face/interface terms, whereas higher-order elements restore richer intra-element residual information.

If one sets aside the explicit mesh scaling powers (h_T and h_F) derived from mathematical trace inequalities, the remaining face term simply measures the nonzero jumps in the tangential field intensity $\mathbf{H}_t$ across element interfaces. This demonstrates that the physical field jump indicators, widely adopted in early engineering practice before the advent of formal *a posteriori* analysis, captured the core mechanism of discretization errors remarkably well and remain highly effective for guiding adaptive mesh refinement.

In a completely parallel manner, for the Ω formulation, the numerical error in the energy norm $\|\mu^{1/2}(\mathbf{H}-\mathbf{H}_h)\|_D$, denoted by $\varepsilon_{\Omega,D}$, is considered. The local residual error estimator for an element T is defined as

$$\eta^2_{\Omega,T} = \eta^2_{\Omega;1} + \sum_{F\subset\partial T}\eta^2_{\Omega;2}, \tag{23}$$

with

$$\eta^2_{\Omega;1} = h_T^2\left\|\mathrm{div}\,(\mu\mathbf{H}_h)\right\|^2_T, \tag{24}$$

$$\eta^2_{\Omega;2} = h_F\left\|[\mu\mathbf{H}_h\cdot\mathbf{n}]_F\right\|^2_F. \tag{25}$$

Comparing (19)–(20) and (24)–(25) offers interesting physical insight: the intrinsic characteristics of dual potential formulations are directly mirrored in the mathematical structure of their residual error estimators. While the $\mathbf{A}$ formulation enforces exact normal continuity of $\mathbf{B}_h$ through curl-conforming spaces and quantifies discretization errors via tangential magnetic field jumps $[\mathbf{H}_h\times\mathbf{n}]_F$, the Ω formulation inherently maintains exact

tangential continuity of $\mathbf{H}_h$ via grad-conforming spaces, shifting the error manifestation entirely to normal flux density jumps $[\mu\mathbf{H}_h \cdot \mathbf{n}]_F$.

Furthermore, a similar structural degeneration occurs when using low-order finite element spaces. When the permeability is piecewise constant, $\operatorname{div}(\mu\mathbf{H}_h)$ vanishes identically inside every element T, rendering the interior residual $\eta_{\Omega;1} \equiv 0$ everywhere. Consequently, the error estimator becomes completely blind to whether the governing equation is truly satisfied in the element interior, placing the entire burden of error indication onto the interface jumps $\eta_{\Omega;2}$. Mirroring the observation in the $\mathbf{A}$ formulation, this collapse again highlights a critical limitation of low-order discretization: low-order elements provide zero interior residual feedback, whereas higher-order spaces restore necessary intra-element sensitivity.

D. Industrial perspectives and practical bottlenecks

Although adaptive mesh refinement and related error-estimation techniques have been incorporated into various commercial CAE packages and industrial codes, their theoretical capabilities do not always translate directly into routine engineering practice.

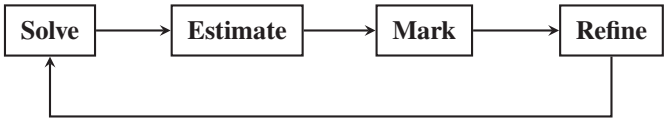


Fig. 1. The standard adaptive mesh refinement loop.

As illustrated in Fig. 1, this loop provides a standard conceptual framework for adaptive mesh refinement. In practice, however, several computational, algorithmic, and software-engineering bottlenecks can limit its routine adoption in industrial workflows.

First, classical error estimators primarily identify *where* the discretization error is concentrated, while translating this information into an efficient refinement strategy remains non-trivial. Many standard h-refinement strategies rely on isotropic element splitting. In regions with highly anisotropic or localized field variation, such as thin skin depth layers and narrow air gaps, or in regions with strong nonlinear field concentration, isotropic refinement can lead to a rapid increase in degrees of freedom (DoFs) without yielding a proportional reduction in error.

Second, from a computational-efficiency standpoint, the main advantage of adaptive mesh refinement is that it can achieve a prescribed accuracy with fewer DoFs than a uniformly refined mesh, and therefore potentially reduce memory consumption. However, this reduction in the number of DoFs does not necessarily translate into lower wall-clock time. Each adaptive iteration incurs overhead associated with error-estimator evaluation, remeshing, system re-assembly, and the potentially reduced effectiveness of previously converged solutions as initial guesses for nonlinear iterative solvers when the mesh topology changes.

Third, software architecture and licensing can present substantial practical barriers. If a commercial CAE package does not natively support error estimation, end-users often have limited ability to integrate custom error-estimation procedures into the native workflow when the underlying software environment is closed or strongly restricted. Even in industrial codes, the meshing pre-processor, the FE solver, and post-processing error analysis are built as independent modules. Dealing with cross-module interfaces, data exchange, and third-party software licensing can make automated loop integration difficult and costly in routine engineering workflows. This is therefore less a mathematical issue than a software-engineering and integration challenge.

At the same time, changes in computing hardware shifted engineering priorities. In the early days of computational electromagnetics, limited RAM and processing power made computational resources scarce, making efficient use of DoFs an important practical consideration and increasing the value of error estimation. As computational resources became more abundant and affordable, direct global mesh refinement became a practical alternative for many applications.

From an operational standpoint, automated adaptive mesh refinement requires the specification of error tolerances, monitoring of mesh quality, and repeated execution of meshing, assembly, and solution procedures. In routine industrial design workflows, these additional steps may be perceived as burdensome, particularly when globally refined meshes are already computationally affordable. In such settings, the pragmatic strategy of "generate an ultra-fine mesh, press the solve button, go grab a cup of coffee, and let the computer run" may become increasingly attractive.

These practical considerations may help explain why *a posteriori* error estimation remains less prominent in routine engineering practice than its theoretical importance might suggest.

III. Emerging needs in the era of data-driven applications

> *"When one door closes, another opens; but we often look so long and so regretfully upon the closed door that we do not see the one which has opened for us."*
>
> – Alexander Graham Bell

As discussed in the previous section, the increase in computing power has made fine-mesh simulations easily affordable, reducing the need for traditional error-driven adaptive mesh refinement in standard single-run solves. However, this same increase in computing power has driven a major shift in how simulations are used: rather than just solving a single case, simulations are now used as data-generation engines to build large-scale datasets.

This shift is closely connected to the rapid emergence of data-driven approaches, particularly deep learning, which have attracted considerable attention across engineering disciplines. It should be emphasized, however, that the success of these approaches relies heavily on the availability of large-scale and diverse datasets. In low-frequency electromagnetics, physical measurement data is often scarce, expensive, or difficult to collect under extreme operating conditions. High-fidelity finite element simulations are therefore used to generate synthetic training data for surrogate models and digital twins.

However, using simulation as a data generator poses a key risk. Numerical simulation errors, such as discretization errors, are not random noise; they are systematic biases. For any downstream surrogate model, the total prediction error combines the surrogate's own approximation error with the underlying numerical error contained in the training data. A surrogate model trained on such data may consequently learn numerical artifacts as part of the underlying input-output relationship.

In safety-critical applications, rapid predictions based on such training data may introduce significant risks. Therefore, *a posteriori* error estimation can play a role beyond mesh adaptation: it can serve as a quantitative data-quality criterion for simulation-generated datasets. Rather than requiring every training sample to be computed on an excessively fine mesh, error estimation can be used to identify samples whose numerical discretization error is sufficiently small for the intended downstream task.

A practical example of this need is the non-destructive testing (NDT) of thin-walled metallic tubes in nuclear power plants, such as steam generator tubes. In practice, linking complex defect morphologies to NDT signatures is difficult because experimental data is scarce; one cannot realistically fabricate and test every crack shape on actual tubing.

Numerical simulation fills this gap by generating the required datasets. Increased computing power now allows finite element models to capture fine geometric details that were previously impossible to simulate, such as the realistic defects shown in Fig. 2, moving beyond simplified canonical shapes [55]. Once validated, these detailed finite element models act as scalable data generators. The generated datasets not only help clarify the link between complex defects and measurement signals, but also provide the essential data foundation for inverse problems, surrogate modeling, and other downstream applications [56].

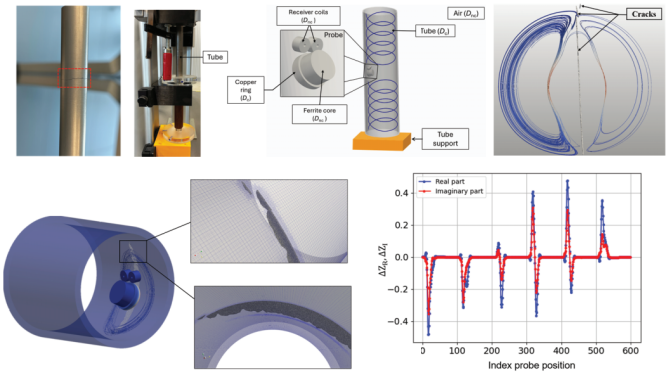


Fig. 2. Finite element modeling of realistic defects with complex geometries in steam generator tubes.

In such applications, global energy-norm errors are rarely the primary concern. Instead, engineers focus on a specific quantity of interest (QoI), such as the local magnetic flux density or impedance change near a defect. A small global error does not necessarily imply high accuracy in the targeted QoI; the relevant quantity is therefore the error in the functional defining the QoI. Moreover, neither global refinement nor simple local mesh refinement near the defect can guarantee high accuracy in the targeted QoI, as illustrated in [57].

To address these needs, a mathematical framework for rigorous QoI error control has recently been established, relying on the solution of an adjoint problem. These approaches provide proven guaranteed error bounds for both static [58] and eddy-current problems [59], yielding rigorous error bounds directly relevant to sensor measurements and engineering decisions. However, QoI-oriented error estimation requires not only an additional global adjoint problem, but also dual formulations to ensure fully guaranteed bounds. This combination drastically increases the overall computational cost, a major bottleneck when performing large-scale 3D simulations.

To overcome this computational bottleneck, one promising approach is to construct these dual solutions locally, an idea that is receiving increasing attention across various computational domains. The key concept is to avoid solving a global dual problem by relying on local constructions. Early theoretical foundations for such local approaches were pioneered by Ern and Vohralík [60], with recent significant extensions to face elements [61] and edge elements [62, 63, 64].

Naturally, there is no free lunch: trading global solves for local reconstructions can lead to less sharp error bounds or a potential loss of precision in the target QoI. Assessing whether these local approaches can achieve the required accuracy for complex electromagnetic QoIs remains an active area of ongoing research.

To close this discussion, this trade-off in dual formulations is illustrated from another angle, using a personal favorite benchmark example: a unit cube domain with a known analytical solution [65]. The main advantage of this benchmark is that, while it is not a realistic physical problem, it strictly follows the magnetostatic formulation with a simple excitation source, allowing the analysis to focus purely on the effect of mesh discretization. In [66], a detailed comparison between residual-based and equilibrated error estimators was conducted. Two main limitations of the equilibrated estimator were highlighted: first, its substantial computational cost arising from the global dual solve; second, its inability to separate the individual error contributions of the primal and dual formulations, as it inherently measures their combined sum.

To demonstrate the impact of high-order dual formulations, take the $\mathbf{A}$-based primal formulation as an example. Constructing its dual solution in a higher-order space $\mathbf{H}_h^{\text{high}}$ alters the balance between the error components in the hypercircle identity:

$$\|\nu^{1/2}(\mathbf{B}-\mathbf{B}_h)\|_D^2+\|\mu^{1/2}(\mathbf{H}-\mathbf{H}_h^{\text{high}})\|_D^2 = \|\nu^{1/2}\mathbf{B}_h-\mu^{1/2}\mathbf{H}_h^{\text{high}}\|_D^2.$$

Because the dual error term $\|\mu^{1/2}(\mathbf{H}-\mathbf{H}_h^{\text{high}})\|_D^2$ decays more rapidly, it becomes negligible. Consequently, the primal error dominates the sum, as illustrated in Fig. 3. This yields a sharper bound that closely mirrors the spatial distribution of the $\mathbf{A}$ formulation error, despite the estimator remaining a sum.

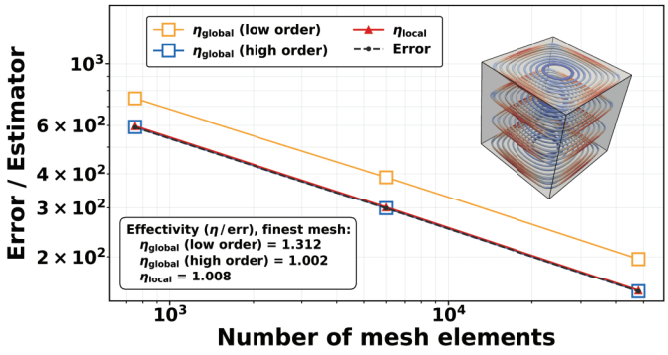


Fig. 3. Exact error of the $\mathbf{A}$ formulation and different estimators as a function of the number of mesh elements.

A similar behavior can be observed in Fig. 4 when considering the Ω formulation, where a high-order dual flux density $\mathbf{B}_h^{\text{high}}$ is constructed.

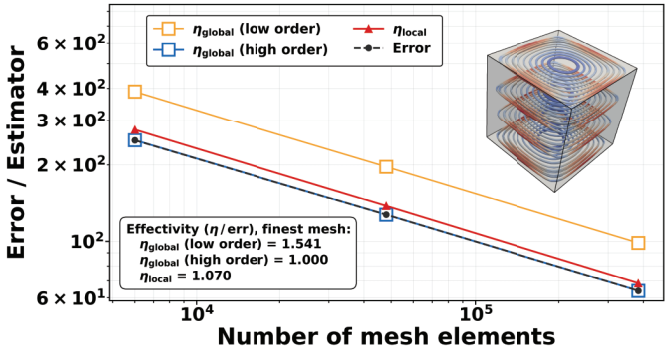
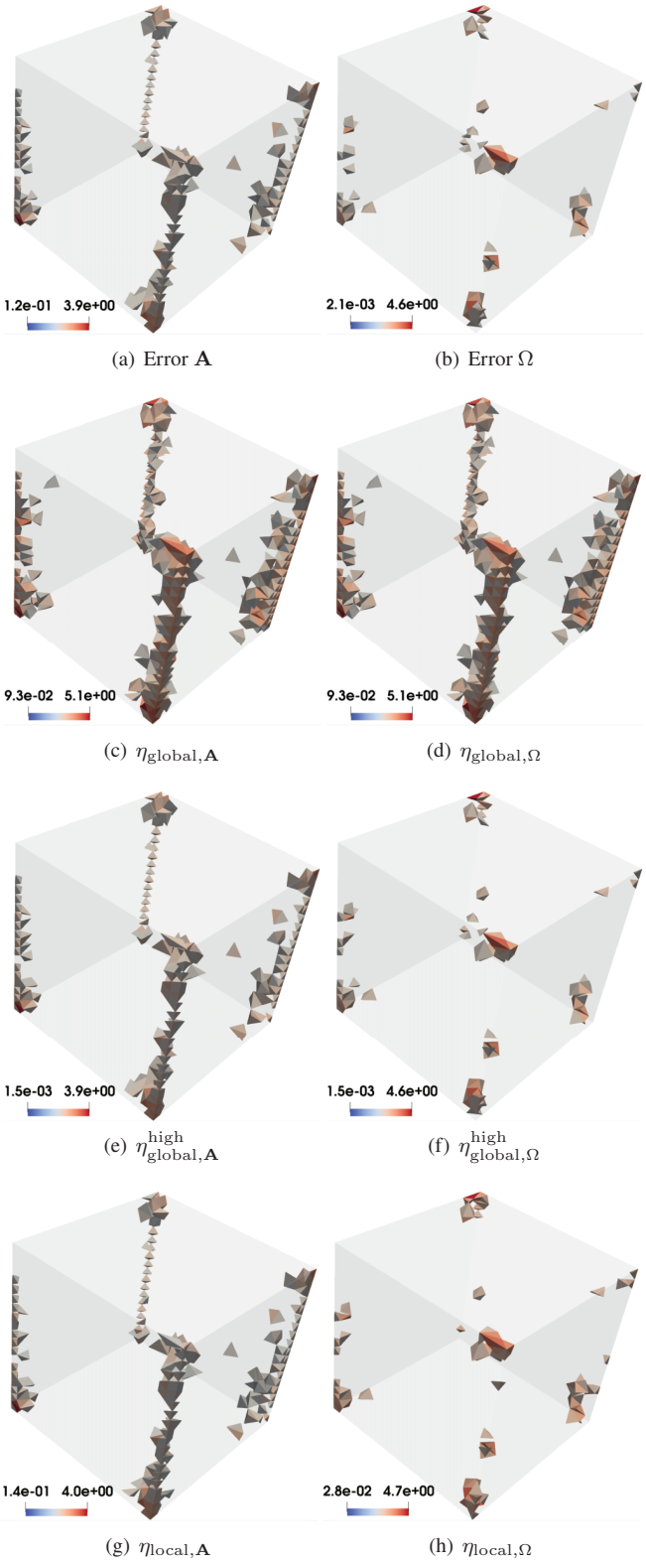


Fig. 4. Exact error of the Ω formulation and different estimators as a function of the number of mesh elements.

Of course, this approach is paradoxical in practice: significantly more expensive computational resources are spent on a high-order dual solve merely to evaluate a cheap, low-order primal solution. Nevertheless, it proves that paying a higher computational cost allows one to recover a sharp error estimate and decoupled error structures.

To provide a complete picture, the performance of local approaches is also demonstrated. As reflected in the effectivity index, the local approach sacrifices a small degree of accuracy in exchange for substantially reduced computational cost.



(a) Error $\mathbf{A}$ (b) Error Ω

(c) $\eta_{\text{global},\mathbf{A}}$ (d) $\eta_{\text{global},\Omega}$

(e) $\eta^{\text{high}}_{\text{global},\mathbf{A}}$ (f) $\eta^{\text{high}}_{\text{global},\Omega}$

(g) $\eta_{\text{local},\mathbf{A}}$ (h) $\eta_{\text{local},\Omega}$

Fig. 5. Spatial distributions of the exact errors and the global and local equilibrated error estimators for the $\mathbf{A}$ and Ω formulations.

The spatial distributions of the true errors and different estimators are presented in Fig. 5. Under a low-order dual formulation, the estimator distributions in Figs. 5(c) and (d), which are indeed identical, fail to distinguish between the two primal formulations or reflect their distinct true error fields shown in Figs. 5(a) and (b). In contrast, using a high-order dual formulation produces the estimator distributions in Figs. 5(e) and (f), which separate and reproduce the distinct spatial error patterns of both formulations. A similar spatial distribution is also obtained using the local approach, showing only minor visible discrepancies compared to the high-order dual formulation.

Finally, looking back at the development of error estimation, the choice has always come down to a practical engineering trade-off.

However, it must be emphasized that even though traditional low-order implementations of equilibrated estimators were computationally heavy and uninformative, failing to isolate individual error contributions, their mathematically guaranteed property remains a fundamental and essential asset. Guaranteed bounds provide a rigorous way to isolate and certify the numerical discretization component, while other uncertainty sources require separate treatment. Given that simulation errors stem from diverse and coupled sources, without sufficiently rigorous bounds, it becomes difficult to reliably assess the relative magnitude of different error sources, such as discretization error, stochastic uncertainties [67], and linear or nonlinear iteration errors [68].

Today, however, advancing computing power has done more than just speed up calculations; it has changed how we view computational costs and redefined what we consider "expensive".

In modern data-driven modeling and digital twins, where simulations serve as tools to generate training data, data reliability directly shapes downstream performance. Although foundational mathematical tools for error separation have long existed, they were often sidelined at the time simply because they were not seen as necessary. The current context, however, perhaps demands a shift in perspective.

Ultimately, the challenge is no longer purely technical; it is also an engineering choice: determining whether, when, how, and at what computational cost these rigorous tools should be deployed.

References

[1] I. Babuška and W. C. Rheinboldt, "Error estimates for adaptive finite element computations," *SIAM Journal on Numerical Analysis*, vol. 15, no. 4, pp. 736–754, 1978.

[2] J. Penman and M. Grieve, "An approach to self adaptive mesh generation," *IEEE Transactions on Magnetics*, vol. 21, no. 6, pp. 2567–2570, 1985.

[3] S.-y. Hahn, C. Calmels, G. Meunier, and J. Coulomb, "A posteriori error estimate for adaptive finite element mesh generation," *IEEE Transactions on Magnetics*, vol. 24, no. 1, pp. 315–317, 1988.

[4] A. Raizer, G. Meunier, and J.-L. Coulomb, "An approach for automatic adaptive mesh refinement in finite element computation of magnetic fields," *IEEE Transactions on Magnetics*, vol. 25, no. 4, pp. 2965–2967, 1989.

[5] P. Fernandes, P. Girdinio, P. Molfino, G. Molinari, and M. Repetto, "A comparison of adaptive strategies for mesh refinement based on a posteriori local error estimation procedures," *IEEE transactions on magnetics*, vol. 26, no. 2, pp. 795–798, 1990.

[6] P. Fernandes, P. Girdinio, P. Molfino, and M. Repetto, "Local error estimates for adaptive mesh refinement," *IEEE transactions on Magnetics*, vol. 24, no. 1, pp. 299–302, 1988.

[7] G. Drago, P. Molfino, M. Nervi, and M. Repetto, "A 'local field error problem' approach for error estimation in finite element analysis," *IEEE Transactions on Magnetics*, vol. 28, no. 2, pp. 1743–1746, 1992.

[8] T. Nehl and D. Field, "Adaptive refinement of first order tetrahedral meshes for magnetostatics using local Delaunay subdivisions," *IEEE Transactions on Magnetics*, vol. 27, no. 5, pp. 4193–4196, 1991.

[9] D. P. Labridis, "Comparative presentation of criteria for adaptive finite-element mesh generation in multiconductor eddy-current problems," *IEEE transactions on magnetics*, vol. 36, no. 1, pp. 267–280, 2000.

[10] D. Ladas, V. Mazauric, G. Meunier, O. Chadebec, M. Ebene-Ebene, Y. Maréchal, and P. Wendling, "An energy based approach of electromagnetism applied to adaptive meshing and error criteria," *IEEE transactions on magnetics*, vol. 44, no. 6, pp. 1246–1249, 2008.

[11] W. Prager and J. L. Synge, "Approximations in elasticity based on the concept of function space," *Quarterly of Applied Mathematics*, vol. 5, no. 3, pp. 241–269, 1947.

[12] P. Ladeveze and D. Leguillon, "Error estimate procedure in the finite element method and applications," *SIAM journal on numerical analysis*, vol. 20, no. 3, pp. 485–509, 1983.

[13] Z. Cendes and D. Shenton, "Adaptive mesh refinement in the finite element computation of magnetic fields," *IEEE Transactions on Magnetics*, vol. 21, no. 5, pp. 1811–1816, 1985.

[14] K. Mitchell and J. Penman, "Self adaptive mesh generation for 3-D finite element calculation," *IEEE Transactions on Magnetics*, vol. 28, no. 2, pp. 1751–1754, 1992.

[15] K. Chellamuthu and N. Ida, "'A posteriori' element by element local error estimation technique and 2D & 3D adaptive finite element mesh refinement," *IEEE Transactions on Magnetics*, vol. 30, no. 5, pp. 3527–3530, 1994.

[16] J. Rikabi, C. F. Bryant, and E. M. Freeman, "An error-based approach to complementary formulations of static field solutions," *International journal for Numerical Methods in Engineering*, vol. 26, no. 9, pp. 1963–1987, 1988.

[17] C. Li, Z. Ren, and A. Razek, "Application of complementary formulations and adaptive mesh refinements to non-linear magnetostatic problems," *IEEE Transactions on Magnetics*, vol. 31, no. 3, pp. 1376–1379, 1995.

[18] F. Marmin, S. Clenet, F. Piriou, and P. Bussy, "Error estimation of finite element solution in nonlinear magnetostatic 2D problems," *IEEE Transactions on Magnetics*, vol. 34, no. 5, pp. 3268–3271, 1998.

[19] J.-F. Remacle, P. Dular, A. Genon, and W. Legros, "A posteriori error estimation and adaptive meshing using error in constitutive relation," *IEEE Transactions on Magnetics*, vol. 32, no. 3, pp. 1369–1372, 1996.

[20] J.-F. Remacle, C. Geuzaine, P. Dular, H. Hedia, and W. Legros, "Error estimation based on a new principle of projection and reconstruction," *IEEE Transactions on Magnetics*, vol. 34, no. 5, pp. 3264–3267, 1998.

[21] Z. Ren and N. Ida, "Derivation of various dual formulations in magnetostatics via error based energy approach," *IEEE transactions on magnetics*, vol. 35, no. 3, pp. 1167–1170, 1999.

[22] G. Marques, S. Clénet, and F. Piriou, "Error estimators in 3D linear magnetostatics," *IEEE transactions on magnetics*, vol. 36, no. 4, pp. 1588–1591, 2000.

[23] Z. Ren, "On the complementarity of dual formulations on dual meshes," *IEEE Transactions on Magnetics*, vol. 45, no. 3, pp. 1284–1287, 2009.

[24] Z. Ren and X. Xu, "Dual discrete geometric methods in terms of scalar potential on unstructured mesh in electrostatics," *IEEE Transactions on Magnetics*, vol. 50, no. 2, pp. 37–40, 2014.

[25] R. Specogna, "One stroke complementarity for Poisson-like problems," *IEEE Transactions on Magnetics*, vol. 51, no. 3, pp. 1–4, 2015.

[26] R. Specogna, "Lean complementarity for Poisson problems," *IEEE Transactions on Magnetics*, vol. 52, no. 3, pp. 1–4, 2016.

[27] Y. Zhao and Z. Tang, "Accurate extraction of winding inductances using dual formulations without source field computation," *IEEE Transactions on Magnetics*, vol. 55, no. 6, pp. 1–4, 2019.

[28] Y. Zhao and Z. Tang, "Improved equilibrated error estimates for open boundary magnetostatic problems based on dual $\mathbf{A}$ and $\mathbf{H}$ formulations," *IEEE Transactions on Magnetics*, vol. 55, no. 6, pp. 1–5, 2019.

[29] M. Schöbinger, J. Schöberl, and K. Hollaus, "An error estimator for multiscale FEM for the eddy-current problem in laminated materials," *IEEE Transactions on Magnetics*, vol. 54, no. 3, pp. 1–4, 2018.

[30] M. Schöbinger, J. Schöberl, and K. Hollaus, "An equilibrated error estimator for the multiscale finite element method of a 2-D eddy current problem," *IEEE Transactions on Magnetics*, vol. 57, no. 6, pp. 1–4, 2021.

[31] M. Schöbinger and K. Hollaus, "An equilibrated error estimator for the 2-D/1-D MSFEM $\mathbf{T}$-formulation of the eddy current problem," *IEEE Transactions on Magnetics*, vol. 60, no. 5, pp. 1–6, 2024.

[32] A. Bossavit, "Complementary formulations in steady-state eddy-current theory," *IEE Proceedings A (Science, Measurement and Technology)*, vol. 139, no. 6, pp. 265–272, 1992.

[33] R. Beck, R. Hiptmair, R. H. Hoppe, and B. Wohlmuth, "Residual based a posteriori error estimators for eddy current computation," *ESAIM: Mathematical Modelling and Numerical Analysis*, vol. 34, no. 1, pp. 159–182, 2000.

[34] S. Nicaise and E. Creusé, "A posteriori error estimation for the heterogeneous Maxwell equations on isotropic and anisotropic meshes," *Calcolo*, vol. 40, no. 4, pp. 249–271, 2003.

[35] S. Cochez-Dhondt and S. Nicaise, "Robust a posteriori error estimation for the Maxwell equations," *Computer methods in applied mechanics and engineering*, vol. 196, no. 25-28, pp. 2583–2595, 2007.

[36] J. Schöberl, "A posteriori error estimates for Maxwell equations," *Mathematics of Computation*, vol. 77, no. 262, pp. 633–649, 2008.

[37] W. Zheng, Z. Chen, and L. Wang, "An adaptive finite element method for the $\mathbf{H} - \psi$ formulation of time-dependent eddy current problems," *Numerische Mathematik*, vol. 103, no. 4, pp. 667–689, 2006.

[38] E. Creusé, S. Nicaise, Z. Tang, Y. Le Menach, N. Nemitz, and F. Piriou, "Residual-based a posteriori estimators for the $\mathbf{A} - \varphi$ magnetodynamic harmonic formulation of the Maxwell system," *Mathematical Models and Methods in Applied Sciences*, vol. 22, no. 05, p. 1150028, 2012.

[39] Z. Tang, Y. Le Menach, E. Creusé, S. Nicaise, F. Piriou, and N. Nemitz, "Residual and equilibrated error estimators for magnetostatic problems solved by finite element method," *IEEE Transactions on Magnetics*, vol. 49, no. 12, pp. 5715–5723, 2013.

[40] E. Creusé, S. Nicaise, Z. Tang, Y. Le Menach, N. Nemitz, and F. Piriou, "Residual-based a posteriori estimators for the $\mathbf{T}/\Omega$ magnetodynamic harmonic formulation of the Maxwell system," *International Journal of Numerical Analysis and Modeling*, vol. 10, no. 2, pp. 411–429, 2013.

[41] J. Chen, Z. Chen, T. Cui, and L.-B. Zhang, "An adaptive finite element method for the eddy current model with circuit/field couplings," *SIAM Journal on Scientific Computing*, vol. 32, no. 2, pp. 1020–1042, 2010.

[42] E. Creusé, S. Nicaise, and Z. Tang, "Helmholtz decomposition of vector fields with mixed boundary conditions and an application to a posteriori finite element error analysis of the Maxwell system," *Mathematical Methods in the Applied Sciences*, vol. 38, no. 4, pp. 738–750, 2015.

[43] C. Chen, E. Creusé, S. Nicaise, and Z. Tang, "Residual-based a posteriori estimators for the potential formulations of electrostatic and time-harmonic eddy current problems with voltage or current excitation," *International Journal for Numerical Methods in Engineering*, vol. 107, no. 5, pp. 377–394, 2016.

[44] E. Creusé, S. Nicaise, and R. Tittarelli, "Space-time residual-based a posteriori estimators for the $\mathbf{A} - \varphi$ magnetodynamic formulation of the Maxwell system," *Computational Methods in Applied Mathematics*, vol. 14, no. 4, pp. 429–460, 2014.

[45] R. Tittarelli, Y. Le Menach, E. Creusé, S. Nicaise, F. Piriou, O. Moreau, and O. Boiteau, "Space-time residual-based a posteriori estimator for the $\mathbf{A} - \varphi$ formulation in eddy current problems," *IEEE Transactions on Magnetics*, vol. 51, no. 3, pp. 1–5, 2015.

[46] Z. Tang, Y. Le Menach, E. Creusé, S. Nicaise, F. Piriou, and N. Nemitz, "Residual based a posteriori error estimators for harmonic $\mathbf{A}/\varphi$ and $\mathbf{T}/\Omega$ formulations in eddy current problems," *IEEE Transactions on Magnetics*, vol. 49, no. 5, pp. 1721–1724, 2013.

[47] P. Dular, Z. Tang, Y. Le Menach, E. Creusé, and F. Piriou, "Comparison of residual and hierarchical finite element error estimators in eddy current problems," *IEEE Transactions on Magnetics*, vol. 50, no. 2, pp. 501–504, 2014.

[48] P. Dular, Y. Le Menach, Z. Tang, E. Creusé, and F. Piriou, "Finite element mesh adaptation strategy from residual and hierarchical error estimators in eddy current problems," *IEEE Transactions on Magnetics*, vol. 51, no. 3, pp. 1–4, 2015.

[49] Z. Tang, Y. Le Menach, E. Creusé, S. Nicaise, and F. Piriou, "Residual a posteriori estimator for magnetoharmonic potential formulations with global quantities for the source terms," *IEEE Transactions on Magnetics*, vol. 51, no. 3, pp. 1–4, 2015.

[50] Z. Tang and Y. Zhao, "Residual-type a posteriori error estimates for 3-D low-frequency stable Maxwell formulations in both frequency and time domains," *IEEE Transactions on Magnetics*, vol. 56, no. 1, pp. 1–4, 2020.

[51] S. Noguchi, T. Naoe, H. Igarashi, S. Matsutomo, V. Cingoski, A. Ahagon, and A. Kameari, "A new adaptive mesh refinement method in FEA based on magnetic field conservation at elements interfaces and non-conforming mesh refinement technique," *IEEE Transactions on magnetics*, vol. 53, no. 6, pp. 1–4, 2017.

[52] S. Noguchi, S. Matsutomo, and V. Cingoski, "An adaptive FEM based on magnetic field conservation applying to ferromagnetic problems," *IEEE Transactions on Magnetics*, vol. 54, no. 3, pp. 1–4, 2018.

[53] R. Tittarelli, Y. Le Menach, F. Piriou, E. Creusé, S. Nicaise, and J.-P. Ducreux, "Comparison of numerical error estimators for eddy-current problems solved by FEM," *IEEE Transactions on Magnetics*, vol. 54, no. 3, pp. 1–4, 2018.

[54] E. Creusé, Y. Le Menach, S. Nicaise, F. Piriou, and R. Tittarelli, "Two guaranteed equilibrated error estimators for harmonic formulations in eddy current problems," *Computers & Mathematics with Applications*, vol. 77, no. 6, pp. 1549–1562, 2019.

[55] B. Cherqaoui, T. Henneron, Z. Tang, J.-P. Ducreux, E. Guillot, and S. Clénet, "Finite element modeling of real defects in thin-walled tubes derived from x-ray tomography," *NDT & E International*, vol. 164, p. 103833, 2026.

[56] B. Cherqaoui, T. Henneron, Z. Tang, S. Clénet, and J.-P. Ducreux, "Analysis of indicator–parameter relationships in eddy current signals for fine Gaussian cracks simulated using the finite element method," *IEEE Transactions on Magnetics*, pp. 1–1, 2026.

[57] Z. Tang, S. Lou, A. Benabou, E. Creusé, S. Nicaise, J. Korecki, and J.-C. Mipo, "Guaranteed quantity of interest error estimate based on equilibrated flux reconstruction," *IEEE Transactions on Magnetics*, vol. 57, no. 6, pp. 1–4, 2021.

[58] E. Creusé, S. Nicaise, and Z. Tang, "Goal-oriented error estimation based on equilibrated flux and potential reconstruction for the approximation of elliptic and parabolic problems," *Computers & Mathematics with Applications*, vol. 146, pp. 323–338, 2023.

[59] E. Creusé, S. Nicaise, and Z. Tang, "Goal-oriented error estimation based on equilibrated flux reconstruction for the approximation of the harmonic formulations in eddy current problems," *IMA Journal of Numerical Analysis*, vol. 45, pp. 126–162, 01 2025.

[60] A. Ern and M. Vohralík, "Adaptive inexact newton methods with a posteriori stopping criteria for nonlinear diffusion pdes," *SIAM Journal on Scientific Computing*, vol. 35, no. 4, pp. A1761–A1791, 2013.

[61] A. Ern, T. Gudi, I. Smears, and M. Vohralík, "Equivalence of local- and global-best approximations, a simple stable local commuting projector, and optimal hp approximation estimates in $H(\mathrm{div})$," *IMA Journal of Numerical Analysis*, vol. 42, pp. 1023–1049, 04 2022.

[62] T. Chaumont-Frelet, A. Ern, and M. Vohralík, "Stable broken $\boldsymbol{H}(\mathrm{curl})$ polynomial extensions and p-robust a posteriori error estimates by broken patchwise equilibration for the curl-curl problem.," *Math. Comput.*, vol. 91, no. 333, pp. 37–74, 2022.

[63] T. Chaumont-Frelet and M. Vohralík, "p-robust equilibrated flux reconstruction in $\boldsymbol{H}(\mathrm{curl})$ based on local minimizations: Application to a posteriori analysis of the curl-curl problem," *SIAM Journal on Numerical Analysis*, vol. 61, no. 4, pp. 1783–1818, 2023.

[64] T. Chaumont-Frelet and M. Vohralík, "A stable local commuting projector and optimal hp approximation estimates in $\boldsymbol{H}(\mathrm{curl})$," *Numerische Mathematik*, vol. 156, no. 6, pp. 2293–2342, 2024.

[65] R. Albanese and G. Rubinacci, "Magnetostatic field computations in terms of two-component vector potentials," *International journal for numerical methods in engineering*, vol. 29, no. 3, pp. 515–532, 1990.

[66] Z. Tang, "Chapter seven - A posteriori error estimates for low frequency electromagnetic computations," in *Error Control, Adaptive Discretizations, and Applications, Part 3* (F. Chouly, S. P. Bordas, R. Becker, and P. Omnes, eds.), vol. 60 of *Advances in Applied Mechanics*, pp. 301–345, Elsevier, 2025.

[67] D. Mac, Z. Tang, S. Clénet, and E. Creusé, "Residual-based a posteriori error estimation for stochastic magnetostatic problems," *Journal of Computational and Applied Mathematics*, vol. 289, pp. 51–67, 2015.

[68] M. Čermák, F. Hecht, Z. Tang, and M. Vohralík, "Adaptive inexact iterative algorithms based on polynomial-degree-robust a posteriori estimates for the Stokes problem," *Numerische Mathematik*, vol. 138, no. 4, pp. 1027–1065, 2018.

Authors name and affiliation

Zuqi Tang

University of Lille

L2EP Laboratory, Bâtiment ESPRIT, Avenue Henri Poincaré, 59655 Villeneuve d'Ascq, France

E-mail: zuqi.tang@univ-lille.fr









